

# Parallel Computation of PDFs on Big Spatial Data Using Spark

Ji Liu<sup>\*1</sup>, Noel Moreno Lemus<sup>†2</sup>, Esther Pacitti<sup>‡1</sup>, Fabio Porto<sup>§2</sup>, and Patrick Valduriez<sup>¶1</sup>

<sup>1</sup>Inria and LIRMM, Univ. of Montpellier, France

<sup>2</sup>LNCC Petrópolis, Brazil

## Abstract

We consider big spatial data, which is typically produced in scientific areas such as geological or seismic interpretation. The spatial data can be produced by observation (*e.g.* using sensors or soil instrument) or numerical simulation programs and correspond to points that represent a 3D soil cube area. However, errors in signal processing and modeling create some uncertainty, and thus a lack of accuracy in identifying geological or seismic phenomenons. Such uncertainty must be carefully analyzed. To analyze uncertainty, the main solution is to compute a Probability Density Function (PDF) of each point in the spatial cube area. However, computing PDFs on big spatial data can be very time consuming (from several hours to even months on a parallel computer). In this paper, we propose a new solution to efficiently compute such PDFs in parallel using Spark, with three methods: data grouping, machine learning prediction and sampling. We evaluate our solution by extensive experiments on different computer clusters using big data ranging from hundreds of GB to several TB. The experimental results show that our solution scales up very well and can reduce the execution time by a factor of 33 (in the order of seconds or minutes) compared with a baseline method.

**Keywords:** Spatial data , big data, parallel processing, Spark

## 1 Introduction

Big spatial data is now routinely produced and used in scientific areas such as geological or seismic interpretation [4]. The spatial data are produced by observation, using sensors [25], [5] or soil instruments [12], or numerical simulation, using mathematical models [6]. These spatial data allow identifying some phenomenon over a spatial reference [9]. For instance, the spatial reference may be a three dimensional soil cube area and the phenomenon a seismic fault, represented as quantities of interest (QOIs) of sampled points (or points for short) in the cube space. The cube area is composed of multiple horizontal slices, each slice having multiple lines and each line having multiple points. A single simulation produces a spatial data set whose points represent a 3D soil cube area.

---

\*ji.liu@inria.fr

†nmlemus@gmail.com

‡esther.pacitti@lirmm.fr

§fporto@lncc.br

¶patrick.valduriez@inria.fr

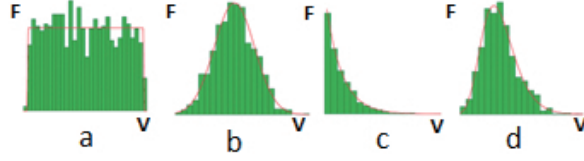


Figure 1: **The distribution of a point.**

However, errors in signal processing and modeling create some uncertainty, and thus a lack of accuracy when identifying phenomena. Such uncertainty must be carefully quantified. In order to understand uncertainty, several simulation runs with different input parameters are usually conducted, thus generating multiple spatial data sets that can be very big, *e.g.* hundreds of GB or TB. Within multiple spatial data sets, each point in the cube area is associated to a set of different observation values in the spatial data sets. The observation values are those observed by sensors, or generated from simulation, at a specific point of the spatial area.

Uncertainty quantification of spatial data is of much importance for geological or seismic scientists [19], [24]. It is the process of quantifying the uncertainty error of each point in the spatial cube space, which requires computing a Probability Density Function (PDF) of each point [13]. The PDF is composed of the distribution type (*e.g.* normal, exponential) and necessary statistical parameters (*e.g.* the mean and standard deviation values for normal and rate for exponential).

Figure 1 shows that the set of observation values at a point may have four distribution types, *i.e.* uniform (a), normal (b), exponential (c), and log-normal (d). The horizontal axis represents the values (V) and the vertical axis represents the frequency (F). The green bars represent the frequency of the observation values in value intervals and the red outline represents the calculated PDF. During the calculation of the PDF at a point, there may be some error between the distribution of the observation values and the calculated PDF. We denote this error by PDF error (or error for short in the rest of the paper). In order to precisely fit a PDF based on observation values, we need to reduce this error. For instance, the set of observation values corresponding to the QOI at a point obeys a normal distribution shown in Figure 1 (b). The mean value of the set of observation values (see Equation 1) may be used as a representative of QOI since it has the highest chance to be the QOI. However, the distribution can be different from normal. And analyzing uncertainty just using the mean or standard deviation values is difficult and imprecise. For instance, if the distribution type of simulated values is exponential (see Figure 1 (c)), we should take the value zero (different from the mean value of the simulated values) as the QOI value since it has the highest possibility. Once we have the PDF of a point, we can calculate the QOI value that has the highest possibility, with which we can compute the imprecision, *i.e.* quantify uncertainty, of each spatial data set.

Calculating the PDF that best fits the observation values at each point can be time consuming. For instance, one simulation of an area of 10km (distance) \* 10km (depth) \* 5km (width) corresponds to 2.4 TB data with 10000 measurements at each point [1]. This area contains  $6.25 * 10^8$  points. The time to calculate the PDF with consideration of 4 distribution types (normal, uniform, exponential and log-normal) can be up to several days or months using a computer cluster.

In this paper, we propose a new solution to efficiently compute PDFs in parallel by taking advantage of Spark [27], a popular in-memory big data processing framework for computer clusters (see [15] for a survey on big data systems). To validate our solution, we use the spatial

data generated from simulations based on the models from the seismic benchmark of the HPC4e project between Europe and Brazil for oil and gas exploration [1]. This benchmark includes models for seismic wave propagation. In oil and gas exploration, seismic waves are sent deep into the Earth and allowed to bounce back. Geophysicists record the waves to learn about oil and gas reservoirs located beneath Earth’s surface.

The problem we address is how to efficiently compute PDFs under bounded error constraints. In addition to deploying PDF computation over Spark, we propose three methods to efficiently compute PDFs: data grouping, machine learning (ML) prediction and sampling. Data grouping consists in grouping similar points to compute the PDF. In the original input data, the data corresponding to some points may be the same or very similar to the data corresponding to a common point. ML prediction uses ML classification methods to predict the distribution type of each point. Sampling method enables to efficiently compute statistical parameters of a region by sampling a fraction of the total number of points to reduce the computation space.

This paper makes the following contributions:

- An architecture to compute PDFs of QOIs in large spatial data sets using Spark.
- Three new methods to reduce the time of computing PDFs, *i.e.* data grouping, ML prediction and sampling.
- An extensive experimental evaluation based on the implementation of the methods in a Spark/HDFS cluster and big data sets ranging from 235 GB to 2.4 TB. The experimental results show that our methods scale up very well and reduce the execution time by a factor of 33 (in the order of seconds or minutes) compared with a baseline method.

The paper is organized as follows. Section 2 introduces some background on Spark. Section 3 gives the problem definition. Section 4 presents our architecture for computing PDFs with Spark, with its main functions. Section 5 presents our solution to compute PDFs in parallel, with three methods, *i.e.* data grouping, ML prediction and sampling. Section 6 presents our experimental evaluation on different computer clusters with different data sizes, ranging from hundreds of GB to several TB. Section 7 concludes.

## 2 Background on Spark

Spark [27] is an Apache open-source data processing framework. It extends the MapReduce model [7] for two important classes of analytics applications: iterative processing (machine learning, graph processing) and interactive data mining (with R, Excel or Python). Compared with MapReduce, it improves the ease of use with the Scala language (a functional extension of Java) and a rich set of operators (Map, Reduce, Filter, Join, Aggregate, Count, etc.). In Spark, there are two types of operations: transformations, which create a new dataset from an existing one (*e.g.* Map and Filter), and actions, which return a value to the user after running a computation on the dataset (*e.g.* Reduce and Count). Spark can be deployed on shared-nothing clusters, *i.e.* clusters of commodity computers with no sharing of either disk or memory among computers. In a Spark cluster, a master node is used to coordinate job execution while worker nodes are in charge of executing the parallel operations.

Spark provides an important abstraction, called resilient distributed dataset (RDD), which is a read-only and fault-tolerant collection of data elements (represented as key-value pairs) partitioned across the nodes of a shared-nothing cluster. RDDs can be created from disk-based resident data in files or intermediate data produced by transformations. They can also be made memory resident for efficient reuse across parallel operations.

Spark data can be stored in the Hadoop Distributed File System (HDFS) [22], a popular open source file system inspired by Google File System [10]. Like GFS, HDFS is a highly scalable, fault-tolerant file system for shared-nothing clusters. HDFS partitions files into large blocks, which are distributed and replicated on multiple nodes. An HDFS file can be represented as a Spark RDD and processed in parallel.

Spark provides a functional-style programming interface with various operations to execute a user-provided function in parallel on an RDD. We can distinguish between operations without shuffling, *e.g.* Map and Filter, and with shuffling, *e.g.* Reduce, Aggregate and Join. Shuffling is the process of redistributing the data produced by an operation, *e.g.* Map, so that it gets partitioned for the next operation to be done in parallel, *e.g.* Reduce. This process is complex and expensive and requires moving data across cluster nodes.

In this paper, we exploit Spark MLlib [2], a scalable machine learning (ML) library that can handle big data [14] in memory by exploiting Spark RDDs and Spark operations. In one method which we propose, we use ML techniques to classify the distribution types of the observation values at different points in order to reduce useless calculation.

### 3 Problem Definition

A spatial data set contains the information to generate an observation value matrix that corresponds to a three dimensional cube area. As a result of running multiple simulations, multiple spatial data sets are produced with a set of observation values at each point. The set of observation values at each point enables the computation of their mean value, standard deviation values and PDF.

Let us illustrate the problem with the spatial data generated from simulations based on the models from the seismic benchmark of the HPC4e project [1]. An important parameter of the models is wave phase velocity, noted  $Vp$  in electromagnetic theory, which is the rate at which the phase of the wave propagates in space. The models contain 16 layers and each layer is associated to a value of  $Vp$ . The top layer delineates the topography and contains the description information of the other 15 layers. Each of the 15 layers is used to generate the observation values of points in a horizontal space of the cube area.

Since our purpose is to study the uncertainty in the output as a result of the wave propagation of the input uncertainty through the model, we assume that the input value of each layer is uncertain and obeys a PDF. The distribution type for every four layers are: Normal, Log-normal, Exponential and Uniform. We use a Monte Carlo method to generate different sets of the 16 input parameters. For each set of input parameters, we generate a spatial data set using the models as shown in Figure 2.

The main problem we address is to efficiently compute PDFs on big spatial data sets, such as the seismic simulation data discussed above. Since it takes much time to compute the PDFs of the points in the whole cube area, our approach is to divide it into multiple spatial regions and compute the PDFs of all the points in a chosen region within a reasonable time. The spatial region is chosen based on some statistical parameters of the region. Thus, the main problem is how to efficiently calculate the PDF of each point in a spatial region, *e.g.* a horizontal slice in the cube area, with a small average error between the PDF and the distribution of the observation values. In order to choose a region, the mean and standard deviation values and the distribution type of a part of the points in the spatial region should be computed. In addition, the average mean value, the average standard deviation value and the percentage of points corresponding to each distribution type in all the points of the region can also be computed. We denote these statistical parameters of a spatial region to compute by the features of a spatial region. A related

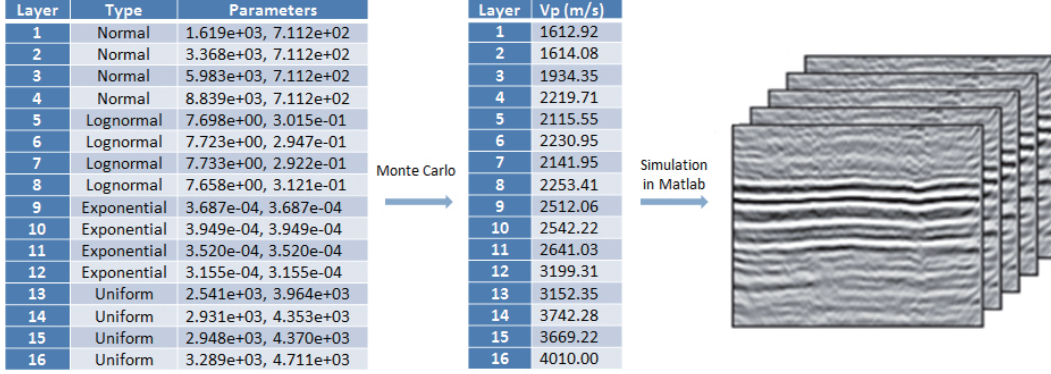


Figure 2: **Data generation from simulation.** This process is repeated multiple times in order to generate multiple data sets. The values of  $Vp$  are different at different iterations.  $Type$  represents the distribution type.

subproblem is how to efficiently calculate the features of a spatial region. In this paper, we take a horizontal slice as a spatial region.

Let  $DS$  be a set of spatial data sets,  $d_k$  be a spatial data set in  $DS$  and  $N$  be the number of points in a region. Each point  $p_{x,y}$ , where  $x$  and  $y$  are spatial dimensions in the slice, has a set of values  $V = \{v_1, v_2, \dots, v_n\}$  while  $v_k$  is the value corresponding to the point  $p_{x,y}$  in  $d_k \in DS$ . Based on these notations, we define Equations 1 - 4 and 6, which are based on the formulas in [8]. The mean  $(\mu_{x,y})$  and standard deviation  $(\sigma_{x,y})$  values of a point can be calculated according to Equations 1 and 2, respectively. And the average mean  $(\bar{\mu}_i)$  and standard deviation  $(\bar{\sigma}_i)$  values of Slice  $i$  can be calculated according to Equations 3 and 4, respectively. The error  $e_{x,y,i}$  between the PDF  $F$  and the set of observation values  $V$  can be calculated according to Equation 5, which compares the probability of the values in different intervals in  $V$  and the probability computed according to the PDF. The intervals are obtained by evenly splitting the space between the maximum value and the minimum value in  $V$ .  $min$  is the minimum value in  $V$ ,  $max$  is the maximum value in  $V$  and  $L$  represents the number of all considered intervals, which can be configured.  $Freq_k$  represents the number of values in  $V$  that are in the  $k$ th interval. The integral of  $PDF(x)$  computes the probability according to the PDF in the  $k$ th interval. Equation 5 is inspired by the Kolmogorov-Smirnov Test [16], which tests whether a PDF is adequate for a data set. In addition, we assume that the probability of the values outside the space between the maximum value and the minimum value is negligible for this equation. Then, the average error  $E$  of Slice  $i$  can be calculated according to Equation 6.

$$\mu_{x,y} = \frac{\sum_{i=1}^n v_i}{n} \quad (1)$$

$$\sigma_{x,y} = \sqrt{\frac{\sum_{i=1}^n (v_i - \mu)^2}{n - 1}} \quad (2)$$

$$\bar{\mu}_i = \frac{\sum_{p_{x,y} \in slice_i} \mu_{x,y}}{N} \quad (3)$$

$$\bar{\sigma}_i = \frac{\sum_{p_{x,y} \in slice_i} \sigma_{x,y}}{N} \quad (4)$$

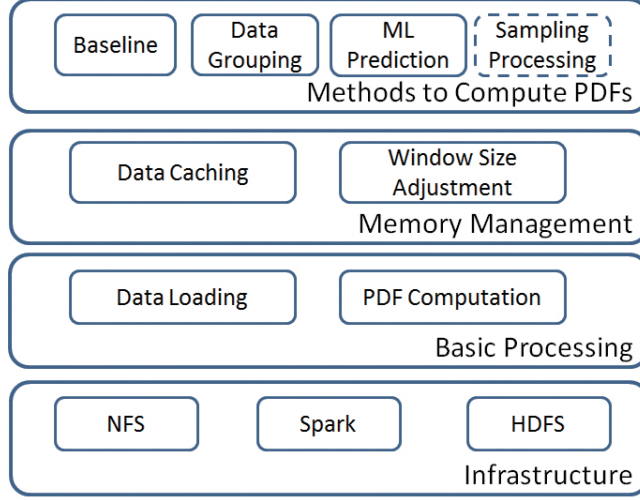


Figure 3: **Architecture for Computing PDFs.**

$$e_{x,y,i} = \sum_{k=1}^N \left| \frac{Freq_k}{N} - \int_{min+(max-min)*\frac{k-1}{L}}^{min+(max-min)*\frac{k}{L}} PDF(x)dx \right| \quad (5)$$

$$E = \frac{\sum_{p_{x,y} \in slice_i} e_{x,y,i}}{N} \quad (6)$$

We can now express the main problem as follows: given a set of spatial data sets  $DS = \{d_1, d_2, \dots, d_n\}$  corresponding to the same spatial cube area  $C = \{slice_1, slice_2, \dots, slice_j\}$ , how to efficiently calculate the mean, standard deviation values and the PDF  $F$  at each point in  $slice_i \in C$  with a small average error  $E$  not higher than a predefined average error  $\varepsilon$ . In addition, we also need to compute the statistical parameters of slices in order to choose Slice  $i$  mentioned in the first subproblem. Thus, the related subproblem can be expressed as: how to efficiently calculate the features of a slice when given the same data sets  $DS$ . The features are:

- $\mu, \sigma$  and distribution type of some points in the slice
- $\bar{\mu}_i, \bar{\sigma}_i$  and the percentage of points for each distribution type in all the points of the slice

## 4 Architecture for Computing PDFs

In this section, we describe the architecture for PDF computation (see Figure 3). This architecture has four layers, *i.e.* infrastructure, basic process to compute PDFs, memory management and methods to compute PDFs. The higher layers take advantage of the lower layers' services to implement their functionality. The infrastructure layer provides the basic execution environment, including Spark, HDFS and Network File System (NFS) in a computer cluster. The basic processing layer provides guiding principles to load the big spatial data and to compute PDFs. The memory management layer allows optimizing the execution of the basic process by caching data and managing sliding windows on big data. The methods to compute PDFs are presented in Section 5.

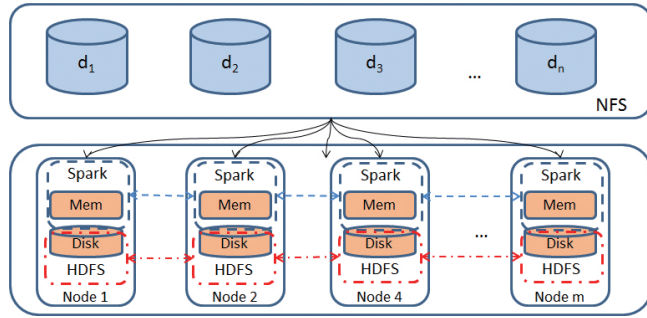


Figure 4: **Infrastructure.**  $d_i$  represents the  $i$ th spatial data set.

## 4.1 Infrastructure with Spark

Figure 4 illustrates the infrastructure we deploy to process big spatial data. The big spatial data is produced by simulation application programs and stored in NFS [21], a shared-disk file system that is popular in scientific applications. Spark and HDFS are deployed over the nodes of the computer cluster. The intermediate data produced during PDF computation and the output data are stored in HDFS, which provides persistence and fault-tolerance.

Keeping the input spatial data in NFS allows us to maximize the use of the cluster resources (disk, memory and CPU), which can be fully dedicated for PDF computation. With the input data stored in NFS, the NFS server is outside the Spark/HDFS cluster and takes care of file management services, including transferring the data that is read to the cluster nodes. An alternative solution would have been to store the input data in HDFS, which would lead to have HDFS tasks competing with Spark tasks for resource usage on the same cluster nodes. We did try this solution and it is much less efficient in terms of data transfer between cluster nodes. This is because HDFS is more complex and does more work due to fault-tolerance and data replication.

We use Spark as our execution environment for computing PDFs. We developed a program written in Scala, which realizes the functionality of different methods to compute PDFs. Once the method to compute PDFs is chosen, the Scala program is executed as a job within Spark.

## 4.2 Principles for the Basic Processing of PDFs

The basic processing of PDFs consists of data loading, from NFS to Spark RDDs, followed by PDF computation using Spark. The data loading process treats the data corresponding to a slice and pre-processes it, *i.e.* calculates statistical parameters of observation values of each point and relates the observation values of each point to an identification of the point. The identification of each point is an integer value which represents the location of the point in the cube area. Then, the PDF computation process groups the data and calculates the PDFs and errors of all the points in a slice based on the pre-processed data. To make the basic processing of PDFs efficient, we use the following guiding principles.

1. **Parallel data loading.** To perform data loading in parallel, we store the identifications of points in an RDD, which is evenly distributed on multiple cluster nodes. For each point in a node, all the corresponding values in different spatial data sets are retrieved from NFS. At the same time, the mean and standard deviation values are calculated. Then, the identification of the point is stored as a key of the point. The mean and standard deviation values and the observations values are stored as the value of the point. The key and value

of the point are stored as a key-value pair in the RDD. This loading process is realized by a Map operation in Spark, which is fully parallel.

2. **Data grouping.** In order to avoid repeating the PDF computation for the same or similar sets of observation values, we group the data of different points that shares similar statistical features, *e.g.* the mean and standard values. Then, a representative point of the group is chosen. The PDF of the representative point is taken to represent all the points in the group. Thus, the PDF computation of all the points in the group is reduced to the computation of the representative point. The grouping can be realized using an *Aggregation* operation in Spark. However, the shuffling process in this operation may take much time. When it takes too much time to group data, we can ignore this principle. After data grouping, the set of the identifications of the points in the group is stored as a part of the value in the key-value pair. For each representative point, the key represents the identification while the value contains the mean and standard deviation values and the observation values.
3. **Parallel processing of PDFs.** The PDF of each point (or representative point) is computed based on its observation values. This process is also realized in a Map operation, which distributes the key-value pairs in RDD of different points to different nodes. Once the PDF of a point is calculated, the error between the observation values and the calculated PDF is computed in the same node. If multiple PDFs of different distribution types are computed, the PDF with the minimum error will be chosen as the PDF of the point. After the parallel processing of PDFs, the key remains the identification of each point (representative point) while the PDF is stored as a part of the value in the key-value pair of the RDD. In addition, since the mean and standard deviation values and the observation values are no longer useful, the corresponding data is removed from the value in the key-value pair. Finally, the PDF of each point is persisted in a file or database system for future use. In addition, an average error of the PDF of the points in the slice is calculated and shown as the result of executing the Scala program.
4. **Sliding window.** Since a slice can have many points that won't fit in memory, we use a sliding window over the slice during data loading, data grouping and parallel processing of PDFs. A window represents a set of points to process, which correspond to several continuous lines in the slice to process. Any two windows have no intersection. After the processing of one window, the process of the next window begins until the end of the slice. Once the size of the window is configured, it stays the same during execution. The size of the window has strong impact on execution and must be chosen carefully (see details in Section 4.3.2).
5. **Use of external programs.** In the parallel data loading and parallel processing of PDFs, we use external programs, which do the specific loading of the points. Since some Java functions, *e.g.* *skipBytes* (Skips and discards a specified number of bytes in the current file input stream), may not work correctly during the parallel execution of a Map operation in Spark [11], we call an external Java program in the Map operation to retrieve observation values of a point from different spatial data sets and pre-process values. Since the PDF computation is implemented by an external program (in R), we call it within the Map operation for the parallel processing of PDFs. Finally, the output data of the external program is transformed to key-value pairs and stored in RDDs by the same Map operation, which executes the external program.



## 4.3 Memory Management

In order to efficiently compute PDFs, we use two memory management techniques to optimize the calculation of PDFs over big data: data caching and window size adjustment.

### 4.3.1 Data Caching

We use data caching, *i.e.* keeping data in main memory, to reduce disk accesses. To identify which data to cache, we distinguish between four kinds of data: input data, instruction data, intermediate data and output data. The input data is the original data to be processed, *i.e.* the big spatial data sets. The instruction data is the data corresponding to the external programs, *e.g.* Java or R programs used in data loading and PDF computation. The intermediate data is the data generated by the data loading process or the execution of external programs, and used by subsequent execution. The output data is the final data generated by the PDF computation.

We use a simple caching strategy. We do not cache input data because it can be very big and read only once. We only cache instruction data and intermediate data, which are accessed much during execution. However, intermediate data that is not used in subsequent operations is removed from main memory. The output data is written to memory first and then persisted.

During execution, some intermediate data that is stored in Spark RDDs can be cached using the Spark *Cache* operation, which stores RDD data in main memory. However, the instruction data of external programs and the intermediate data directly generated by executing these external programs are outside of RDDs. We cache this data in temporary files in memory, using a memory-based file system [23]. Then, the information in the cached files is retrieved and stored as intermediate data in RDDs, which can be again cached using the *Cache* operation of Spark.

### 4.3.2 Window Size Adjustment

The size of the sliding window is critical for efficient PDF computation. When it is too small, the degree of parallel execution among multiple cluster nodes is low. Increasing the window size increases the degree of parallelism, but may introduce some overhead in terms of data transfers among nodes or management of concurrent tasks. Thus, it is important to find an optimal window size in order to make a good trade-off between the degree of parallelism and overhead.

To find the optimal window size, we distinguish between the data loading process and the PDF computation process, which have different data access patterns. In data loading, the processing of each point can be done independently by a Map operation in parallel. Thus, the overhead of data transfers and concurrent task management with a big window size is small. Thus, we can choose a window size that ensures that there is enough work to do for each node and that multiple nodes can be used. For instance, consider a computer cluster with  $n$  nodes, each node with  $c$  CPU cores. Assuming that the data loading for each point can occupy a CPU core, we can choose a maximum window size corresponding to  $n*c$  points. If the number of points is less than  $n*c$ , we choose the maximum number of points as the window size.

During PDF computation, the overhead of having a big window can be high since the processing of different points are not independent especially when we use data grouping. For instance, when the size of window is bigger, the data of more points is present at node. In order to group data, the data of each point need to be compared with the data of more points, which takes more time. In addition, there is much more data transferred among different nodes in the data shuffling process of data grouping. Furthermore, since the PDF computation takes much time, the management of concurrent tasks within each node also increases execution time for a big window. As a result, the overhead of having a big window becomes high for PDF computation.

To find an optimal window size, we test the Scala program on a small workload (with a small number of points) with different window sizes, and then use the optimal size for the PDF computation of all the points in the slice.

## 5 Methods to Compute PDFs

In this section, we present our methods to compute PDFs efficiently. First, we introduce a baseline method, which will be useful for comparison. Then, we propose two methods, *i.e.* data grouping and ML prediction, to compute PDFs, which addresses the main problem defined in Section 3. Finally, we propose a sampling method to calculate the features of a slice, which addresses the related problem.

### 5.1 Baseline Method

The baseline method computes the PDF of each point in a slice as follows (see Algorithm 1). Line 2 loads the spatial data sets and calculates the mean and standard deviation values of each point by using Algorithm 2. Lines 3 - 13 compute the PDF for all the points in the  $i$ th slice. Line 5 gets a window in the slice. Line 6 selects all the points in the window to process. For each point in the window, Line 8 computes the PDF based on the observation values and the error between the PDF and the observation values. This can be achieved by executing an R program. The loop of Lines 7-10 can be executed in parallel using the Map operation in Spark. The *ComputePDF&Error* function is realized by Algorithm 3. The data is persisted in the storage resources (Line 11) and the average error  $E$  is calculated (Line 14). Lines 3-14 correspond to the PDF computation process.

---

#### Algorithm 1 PDF computation

---

**Input:**  $DS$ : a set of spatial data sets corresponding to a spatial cube area;  $i$ : the  $i$ th slice to analyze

**Output:**  $PDF$ : the PDF of all the points in the  $i$ th slice of the cube area;  $E$ : the average error between the PDF and the observation values of all the points in the  $i$ th slice

```

1:  $PDF \leftarrow \emptyset$ 
2:  $RawData \leftarrow loadData(DS, i)$ 
3: while not all points in  $slice_i$  are processed do
4:    $PDF \leftarrow \emptyset$ 
5:    $window \leftarrow GetNextWindow(slice_i)$ 
6:    $Points \leftarrow Select(window, RawData)$ 
7:   for each  $p \in Points$  do
8:      $(pdf, error) \leftarrow ComputePDF\&Error(p, RawData)$ 
9:      $pdfs \leftarrow pdf \cup wsf$ 
10:  end for
11:   $persist(pdf)$ 
12:   $PDF \leftarrow PDF \cup pdfs$ 
13: end while
14:  $E \leftarrow Average(error)$ 
end

```

---

Algorithm 2 loads and preprocesses the spatial data. Line 4 chooses a window to load the data. Then, for each point in the window, the data in each data set of  $DS$  is loaded (Lines

6-10). This process is realized in a Map function in Spark. A Java program is called in the Map function to read the data at a specific position instead of loading all the data. Then, the mean and standard deviation values are calculated (Lines 11 and 12). Finally, the loaded data is cached in memory in a Spark RDD (Line 16).

---

**Algorithm 2** Data loading

---

**Input:**  $DS$ : a set of data sets corresponding to a spatial cube area;  $i$ : the  $i$ th slice to analyze  
**Output:**  $RawData$ : mean, standard deviation and the original data set of each point in the cube area

```

1:  $RawData \leftarrow \emptyset$ 
2: while  $RawData$  does not contain all the points in  $slice_i$  do
3:    $windowData \leftarrow \emptyset$ 
4:    $window \leftarrow GetNextWindow(slice_i)$ 
5:   for each  $p \in window$  do
6:      $rd \leftarrow \emptyset$ 
7:     for each  $ds \in DS$  do
8:        $data \leftarrow GetData(ds, p, i)$ 
9:        $rd \leftarrow data \cup rd$ 
10:    end for
11:     $\mu \leftarrow ComputeMean(rd)$ 
12:     $\sigma \leftarrow ComputeStd(rd)$ 
13:     $rd \leftarrow \mu \cup \sigma \cup rd$ 
14:     $windowData \leftarrow rd \cup windowData$ 
15:  end for
16:   $Cache(windowData)$ 
17:   $RawData \leftarrow windowData \cup RawData$ 
18: end while
end

```

---

Algorithm 3 computes the PDF of a point with the smallest error in a set of candidate distribution types. Line 3 calculates the statistical parameters of PDFs based on different distribution types in a set of distribution candidates  $Types$ . For instance, the parameters for normal are mean and standard deviation values while the parameter for exponential is rate. The more types are considered in  $Types$ , the longer the execution time of Algorithm 3 is. Then, the corresponding error of the PDF based on  $type$  and  $parameters$  are calculated using Equation 5. Finally, the PDF that incurs the smallest error is chosen (Line 7).

We exploit Algorithms 1 and 2 in both the data grouping and ML prediction methods. However, the *Select* and *ComputePDF&Error* functions are different in different methods.

## 5.2 Data Grouping

Some points may have the same distribution of observation values. Thus, using the data grouping method, we can execute the PDF computation process only once and use the result to represent all the corresponding points. In this method, the *Select* function in Algorithm 1 has two steps. First, the points with exactly the same mean and standard deviation values are aggregated into a group. The grouping can be realized by the *aggregation* operation in Spark. Then, one point in each group is selected to represent the group of points. Then, the data corresponding to selected points are processed to compute the PDFs.

---

**Algorithm 3** PDF computing

---

**Input:**  $d$ : a set of observation values for a point;  $Types$ : a set of distribution types  
**Output:**  $PDF$ : the PDF of the point;  $error$ : the error between the PDF defined by the distribution type and the statistical parameters and the observation values of the point

- 1:  $results \leftarrow \emptyset$
- 2: **for each**  $type \in Types$  **do**
- 3:      $parameters \leftarrow fitDistribution(d, type)$
- 4:      $pError \leftarrow CalculateError(type, parameters, d)$  ▷ According to Equation 5
- 5:      $results \leftarrow \{(type, parameter, pError)\} \cup results$
- 6: **end for**
- 7:  $(PDF, error) \leftarrow GetSmallestError(results)$

**end**

---

In some cases, although some points may share the same PDF, the observation values of the points are slightly different. And the mean and standard values may differ by a very small fluctuation. In this case, we can cluster the points that have similar mean and standard deviation values with an acceptable error.

When the number of nodes in the cluster is small and the window size is small, there is few data to be transferred for the grouping. And the grouping method can avoid repeated execution on the same set of observation values. However, when the number of nodes is high or the window size is big, there is much more data to be transferred among different nodes, which may take much time. In some situations, the time to transfer the data may be longer than the time to run the repeated execution. In addition, if a point corresponds to big amounts of data (many observation values), even though the window size is small, the shuffling process of data grouping may also take much time. In this case, the data grouping method is not efficient.

### 5.2.1 Reuse Optimization

When there are points of the same mean and standard deviation values in different windows, we can reuse the existing calculated results in order to avoid new executions. Thus, we propose the reuse optimization method, which not only aggregates the data to groups but also checks if there are already existing results, *i.e.* the PDFs for the point of the same mean and standard deviation values, generated from the previous execution of processed windows. We expect this method to be better than data grouping only. However, it may take time to store all the calculated results and to search existing PDFs from a large list of previously generated results. This extra time may be longer than the reduced time, *i.e.* the time to compute the PDF on the data set (the execution time of Algorithm 3).

## 5.3 ML Prediction

In this section, we propose an ML prediction method based on a decision tree to compute PDFs. Decision tree classifier [20] is a typical ML technique to classify an object into different categories. The basic idea is to break up a complex decision into a union of several simpler decisions, hoping the final solution obtained this way would resemble the intended desired solution. The decision tree can be described as a tree selected from a lattice [3]. A tree  $G = (V, E)$  consists of a finite, nonempty set of nodes  $V$  and a set of edges  $E$ . A path in a tree is a sequence of edges. If there is a path from  $v$  to  $w$  ( $vw$ ), then  $v$  is a proper ancestor of  $w$ ,  $w$  is a proper descendant of  $v$  and the path contains an entry edge for  $w$  and an out edge for  $v$ .

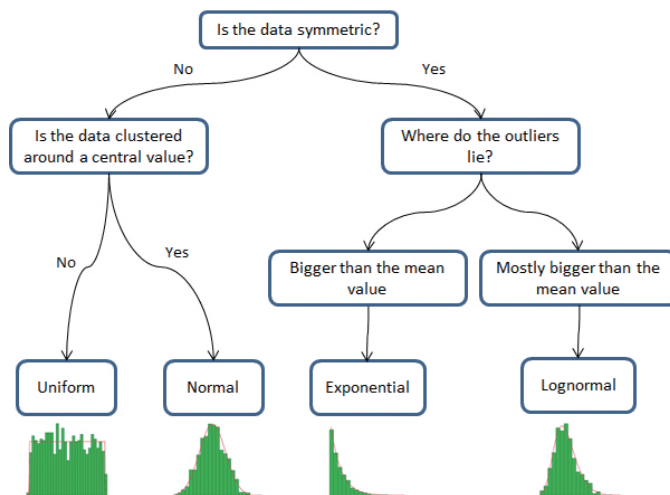


Figure 5: A decision tree to choose the distribution type for a set of data.

A tree has only one root node that does not have any entry edge and all the other nodes have only one entry edge. Each node has only one path from the root. The depth of the graph in a tree is the length of the largest path from the root to a leaf. A leaf is the node that has no proper descendant. The data to be used to generate a decision tree is training data. In order to generate a decision tree, the training data can be split into different data sets (bins) according to different features and each data set is a unit to be processed. The maximum number of bins is defined in order to reduce the time to generate a decision tree. Figure 5 shows a decision tree of depth 3 to choose a distribution type for a data set. However, in this paper, we take some statistical features as parameters to choose a distribution as explained below.

In Algorithm 3, the execution of Lines 3-5 is repeated several times (the number of distribution type candidates), which is very inefficient. We assume that we can learn the correlation among statistical features, *e.g.* mean and standard deviation values, and the distribution type. Then, we can directly predict the distribution type based on the relationship and use the predicted distribution type to execute Lines 3-5 in Algorithm 3 once for each point.

We assume that we have some previously generated output data, which contains the results of several points, *i.e.* the mean and standard deviation values and the type of distribution. Before execution of our method, we can generate a ML model (that correlates between statistical features and distribution types), *i.e.* decision tree, based on the previous existing data. Then, we use Algorithm 4 to replace Algorithm 3.

When the points in the current slice have the same correlation between the statistical features and the distribution types as that in the previously generated output data, we can use ML prediction. Generally, the points in different slices but corresponding to the same spatial data set have the same correlation. Thus, we can use the output data generated based on some points in one slice, *e.g.* Slice 0, to generate decision tree model and use the model to calculate PDFs of the points in other slices, *e.g.* Slice 201.

In addition, since the ML approach optimizes the *ComputePDF&Error* function, it can be combined with other methods. Thus, we call the pure adoption of ML: ML or baseline + ML; the combination of data grouping and ML: data grouping + ML or grouping + ML; the combination of reuse and ML: reuse + ML. Grouping + ML first uses the data grouping methods to group points and then use ML prediction to calculate PDF and error for each representative point.

Reuse + ML first groups the points using the data grouping method and then searches the PDF corresponding to the set of the mean and standard deviation values of each representative point in the results generated by previous execution. If there is no results for the set of mean and standard deviation values, it uses the ML method to calculate the PDF and the error.

---

**Algorithm 4** PDF computing based on ML prediction

---

**Input:**  $d$ : a vector of observation values for a point;  $model$ : the decision tree;  $\mu$ : the mean value of  $d$ ;  $\sigma$ : the standard deviation value of  $d$

**Output:**  $T$ : the distribution type of the point;  $P$ : the parameters of the distribution;  $error$ : the error between the PDF defined by the distribution type and the parameters of the distribution and the real distribution of data in  $d$

1:  $T \leftarrow predict(model, \mu, \sigma)$

2:  $P \leftarrow fitDistribution(d, type)$

3:  $error \leftarrow CalculateError(type, parameter, d)$

▷ According to Equation 5

**end**

---

### 5.3.1 ML Model Generation

In order to generate the decision tree model, there are some hyper-meters to determine, *e.g.* the depth of the tree (*depth*) and the maximum number of bins (*maxBins*). In order to tune the hyper-meters, we randomly split the previously generated output data into two data sets, *i.e.* training set and validation set. We use the training set to train the model with different combinations of hyper-meters. Then, we test the generated models on the validation set in order to choose an optimal combination of hyper-meters. We take the wrong prediction rate in the validation set as the model error while tuning the hyper-meters. The model error represents the preciseness of the decision tree model.

The model error decreases at the beginning and then increases, because of overfitting [26], as the values of *depth* and *maxBins* increase. While the time to train the model becomes longer when the values of *depth* and *maxBins* increase. We choose the minimum values of *depth* and *maxBins*, from which the error does not decrease when they (*depth* or *maxBin*) increase. The process to tune the hyper-meters can take much time. We assume that the points in different slices have the same correlation between the statistical features and distribution types. We also assume that the hyper-meters can be shared to train the models based on different previously generated output data in order to avoid tuning the hyper-meters and to reduce the time to train the decision tree model. Thus, the chosen values of *depth* and *maxBins* are used as fixed hyper-meters to generate the decision tree model for different previously generated output data.

Within the previously generated output data, each point has mean and standard deviation values and the distribution type. Since we have fixed hyper-meters, we do not need to use a validation data set to tune the hyper-meters. Thus, in order to generate the model, we randomly partition the previously generated output data set into two parts, *i.e.* training set and test set. In the training processing, we train the model using the training set. The input of the trained model is the mean and standard values and the output is a predicted distribution type. After generating the model, we take the wrong prediction rate in the test set as the model error while training models. During the PDF computation process, the generated model is broadcast to all the nodes, which reduces communication cost. .

There are scenarios in which the mean and standard deviation share the same values, respectively, but the distribution type is different. In this situation, we can take into consideration

other normalized moments <sup>1</sup>, *e.g.* 3th, 4th etc. However, it may take additional time to calculate other normalized moments. Thus, we only consider the mean and standard deviations. We will experiment with data sets where the points of the same set of mean and standard deviation values have the same distribution types.

## 5.4 Sampling

In order to choose a slice to compute PDFs, we need to compute the features of a slice very quickly. We propose a sampling method (see Algorithm 5) that samples the points and uses ML prediction to generate the distribution type of each point. This method does not run the statistical calculation of the each point in the *ComputePDF&Error* function in Algorithm 1 in order to reduce execution time.

In Algorithm 5, Line 2 samples the points in slice  $i$  based on a predefined sampling rate. A sampling rate represents the ratio between the selected points from the sampling process and all the original points. Lines 4-14 implement the process that loads the data from the data sets and calculates the mean and standard deviation values for each double sampled point. Line 15 groups the data as explained in Section 5.2. When the number of nodes in the cluster is high, we can remove Line 15 in order to reduce the time of shuffling. Lines 17 -20 calculate the distribution type of each double sampled point based on a decision tree (see Section 5.3.1 for details). Lines 22-26 calculate the final results, *i.e.* the average mean value, the average standard deviation and the percentage of different distribution types. Lines 17 - 26 correspond to the PDF computation process.

We can randomly sample the points. The random sampling method takes very time while the selected points may contain little repeated information. We could also use a k-means clustering algorithm [18] and choose the point that is the closest to the center of each cluster as double sampled points. The double sampled data generated by k-means contains diverse information, which does not help much to choose a slice (see details in Section 6.2.3). Furthermore, k-means may take much time to converge. Therefore, instead of k-means, we use random sampling in Algorithm 5.

## 6 Experimental Evaluation

In this section, we evaluate and compare the different methods presented in Section 5 for different data sets and cluster sizes. To ease reading, we call each method by a name as: Baseline, Grouping, Reuse, ML and Sampling. First, we introduce the experimental setup, with two different computer clusters (a small one and a big one). Then, we perform experiments with a 235 GB data set. Finally, we perform experiments with big data sets (1.9 TB and 2.4 TB).

### 6.1 Experimental Setup

In this section, we present the different spatial data sets, the candidate distribution types (see Algorithms 3 and 5) and the cluster testbeds, which we use in our various experiments.

To generate the spatial data, we use the UQlab framework [17] to produce 16 values as the input parameters, *i.e.*  $Vp$ , of the models from the seismic benchmark of the HPC4e project

---

<sup>1</sup>The  $n$ th moment is defined as:

$$\mu_n = \sum_{i=1}^m (x_i - \mu)^n \quad (7)$$

where  $m$  is the number of values in the data set,  $x_i$  is the  $i$ th value in the data set and  $\mu$  is the mean value of the data set.

---

**Algorithm 5** Sampling process

---

**Input:**  $DS$ : a set of data sets produced by simulations;  $i$ : the  $i$ th slice to analyze;  $model$ : the decision tree corresponding to the relationship between the mean and standard value and the distribution type;  $Types$ : a set of distribution types;  $rate$ : the sampling rate

**Output:**  $\bar{\mu}$ : the average mean value of the slice;  $\bar{\sigma}$ : the average standard deviation of the slice;  $TypesPercentage$ : the percentage of distribution types of the points in the slice

```
1:  $SF \leftarrow \emptyset$ 
2:  $Points \leftarrow Sample(slice_i, rate)$ 
3:  $RawData \leftarrow \emptyset$ 
4: for each  $p \in points$  do
5:    $rd \leftarrow \emptyset$ 
6:   for each  $ds \in DS$  do
7:      $data \leftarrow GetData(ds, p, i)$ 
8:      $rd \leftarrow data \cup rd$ 
9:   end for
10:   $\mu \leftarrow ComputeMean(rd)$ 
11:   $\sigma \leftarrow ComputeStd(rd)$ 
12:   $rd \leftarrow \mu \cup \sigma \cup rd$ 
13:   $RawData \leftarrow rd \cup RawData$ 
14: end for
15:  $Points \leftarrow selectByGrouping(RawData)$ 
16:  $allTypes \leftarrow \emptyset$ 
17: for each  $p \in Points$  do
18:    $type \leftarrow predict(model, RawData)$ 
19:    $allTypes \leftarrow type \cup allTypes$ 
20: end for
21:  $TypesPercentage \leftarrow \emptyset$ 
22: for each  $type \in Types$  do
23:    $pct \leftarrow calculatePercentage(type, allTypes)$ 
24:    $TypesPercentage \leftarrow pct \cup TypesPercentage$ 
25: end for
26:  $(\bar{\mu}, \bar{\sigma}) \leftarrow averageCalculation(RawData)$ 
end
```

---



[1]. The input parameters obey four distribution types, *i.e.* normal, exponential, uniform and log-normal. In each simulation, we generate a set of the input parameters according to the PDF of each layer and generate a spatial data set by using the set of the input parameters and the models. We run the simulation multiple times and generate three sets of spatial data sets, denoted by *Set1*, *Set2* and *Set3*. The simulation is repeated 1000 times to generate *Set1*. *Set1* contains 1000 files, each of which is a spatial data set and has 235 GB. In *Set1*, the dimension of the cube area is  $251 * 501 * 501$ , *i.e.* 501 slices, each slice has 501 lines and each line is composed of 251 points. To generate *Set2*, we run the simulation 1000 times while the dimension is  $501 * 1001 * 1001$ . *Set2* has 1.9 TB. A point is associated to 1000 observation values in both *Set1* and *Set2*. Finally, we run the simulation 10000 times with the dimension of  $251 * 501 * 501$  in order to generate *Set3*, which has 2.4 TB. In this data set, a point is associated to 10000 observation values. We use the same slice (Slice 201 because it has interesting information) in all the experiments. We consider two sets of candidate distribution types *Types*, introduced in Algorithms 3 and 5. The first set is the set of distribution types of the input parameters, *i.e.* normal, exponential, uniform and log-normal, since we assume that the distribution types of different points are within those of the input parameters of the simulation. In addition, we assume that the distribution types may belong to other types beyond the scope of the distribution types of the input parameters because of non-linear relationship between the input parameters and the values of each point of the spatial cube area. With this assumption, we have a second type of candidate distribution types, *i.e.* normal, exponential, uniform, log-normal, Cauchy, gamma, geometric, logistic, Student’s t and Weibull. We call the first set 4 – *types* and the second 10 – *types*.

We use two cluster testbeds, each with NFS, HDFS and Spark deployed. The first one, which we call LNCC cluster, is a cluster located at LNCC with 6 nodes, each having 32 CPU cores and 94 GB memory. The second one is a cluster of Grid5000, which we call G5k cluster, with 64 nodes, each having 16 CPU cores and 131 GB of RAM storage.

## 6.2 Experiments on a 235 GB Data Set

In this section, we compare the different methods based on the spatial data set *Set1* of 235 GB. First, we compare the performance of different methods using the LNCC cluster: Baseline, Grouping, Reuse and the combination of these methods with ML. Then, we study the scalability of different methods using the G5k cluster. Finally, we study the performance of Sampling.

We take the relationship between the set of mean and standard deviation values and the distribution types of 25000 points in Slice 0 in the previously generated output data of *Set1* to tune the hyper-meters of the decision tree. The hyper-meters are tuned at the very beginning, which takes 18 minutes for 4 – *types* and 22 minutes for 10 – *types* using Spark on a workstation with 8 CPU cores and 32 GB of RAM.

We take advantage of the previously generated output data of *Set1* to generate the decision tree model for the experiments of this section. The model error is 0.03 for 4 – *types*, and 0.08 for 10 – *types*. Although the model error of 10 – *types* is bigger than that of 4 – *types*, the average error  $E$  in Algorithm 1 is smaller. The time to train the model ranges from 1 to 20 seconds, which is negligible compared with the execution time of the whole PDF computation process.

### 6.2.1 Performance Comparisons

In this section, we compare the performance of different methods, *i.e.* Baseline, Grouping, Reuse, and the combination with ML, using the LNCC cluster. First, we execute the Scala program (for computing PDFs with different methods) on a small workload (6 lines and 3006 points).

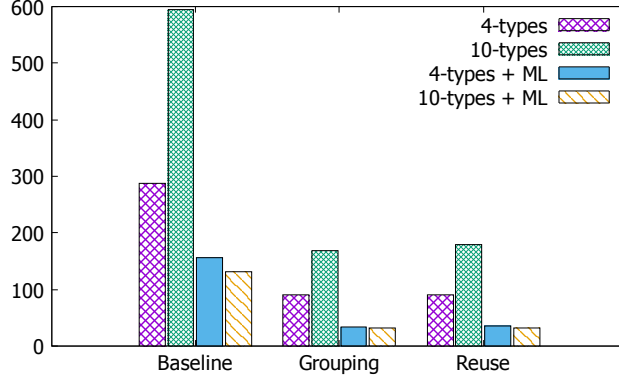


Figure 6: **Execution time for PDF computation on a small workload (6 lines and 3006 points) with 235 GB input data.** The time unit is second.

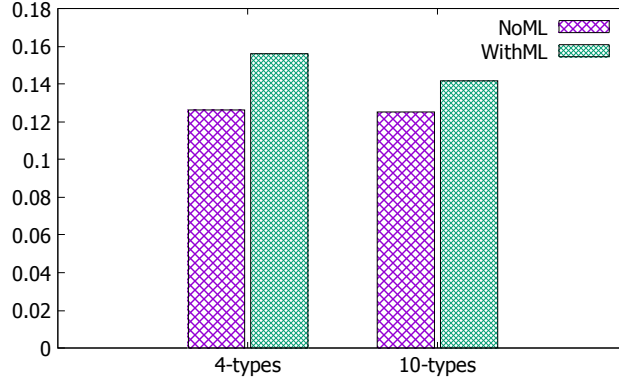


Figure 7: **Error in PDF computation.** NoML represents the error of different methods without adoption of ML, *i.e.* Baseline, Grouping and Reuse with 4 – types or 10 – types (see Figure 6). WithML represents the combinations of methods with ML, *i.e.* Baseline + ML, Grouping + ML, Reuse + ML with 4 – types or 10 – types (see Figure 6).

Second, we compare the performance of different methods for different window sizes. Finally, we compare the performance of different methods with the tuned window size for the whole slice.

**Experiments with Small Workload** In this section, we use a small workload of 6 lines, *i.e.* 3006 points, to compare the performance of different methods. The execution time for PDF computation is shown in Figure 6 and the error is shown in Figure 7.

We execute the program for the points of the first 6 lines in Slice 201 using Baseline, Grouping, Reuse, ML and the combination of these methods with ML. We take 3 lines as a window for PDF computation and we process the data of the points in two windows. The execution time for data loading (see Algorithm 2) is 67s, which is the same for all the methods since we use the same algorithm.

Figure 6 shows the good performance of our methods: Grouping (without Reuse), Reuse and ML. The execution time of Baseline with 10 – types is much longer than that with 4 – types. This is expected since the complexity of Algorithm 3 is  $O(n)$ , with  $n$  distribution types, and

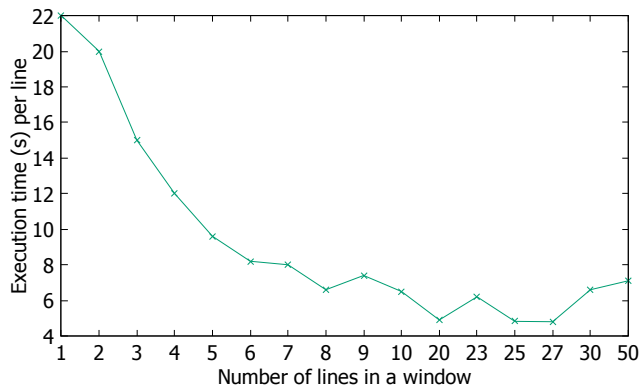


Figure 8: **Average execution time per line for PDF computation with two windows.**

the execution time increases with  $n$ . However, with ML, the execution time is significantly reduced (46% for 4 – types and 78% for 10 – types). If we use Grouping without ML or Reuse, the execution time is also reduced a lot (69% for 4 – types and 72% for 10 – types). This shows that there are many points that obey the same distribution and have the same mean and standard deviation values. In addition, since the data size corresponding to a point is small, *i.e.* 1000 observation values, the shuffling time for computing the aggregation function is short. Thus, Grouping outperforms Baseline much. When we couple Grouping and ML, the advantage becomes more obvious. The combined method is 88% and 95% better compared with the Baseline for 4 – types and 10 – types, *i.e.* the combined method is up to more than 17 times better than Baseline. Reuse is slightly worse than Grouping, but it is still much better than Baseline. This is expected since it takes more time to search for the existing results than to compute PDFs. The difference between Grouping and Reuse is small when the workload is small but it can be significant for bigger workloads.

Figure 7 shows the average error ( $E$  in Equation 6) corresponding to different methods. In Figure 7, we distinguish between the methods that do not use ML, *i.e.* Baseline, Grouping and Reuse, which we call NoML, and those that do exploit ML, *i.e.* Baseline with ML, Grouping with ML and Reuse with ML, which we call WithML. The methods NoML and WithML have the same error for the same distribution type set.

The figure shows that 10 – types does not reduce much the average error for Baseline (up to 0.0013). However, PDF computation may take more time when we consider 10 – types as shown in Figure 6. The average error is higher for WithML than NoML. The difference is small (up to 0.017) but WithML can reduce much the execution time of the PDF computation. In addition, Figure 7 shows that 10 – types leads to a smaller average error, even though the model error is higher for WithML. This is reasonable since there are some types that are very difficult to distinguish in 10 – types but the wrong classification of the distribution types does not increase much the average error. In addition, with more distribution candidate types, the decision tree produces a better classification.

**Window Size Adjustment** The window size is critical for the PDF computation with Grouping. To adjust the window size, we conduct the following experiment. We execute the Scala program with Grouping (with 4 – types and without ML prediction) for two windows while each window is composed of different numbers of lines. Then, we choose a window that corresponds to the shortest average execution time of each line. Figure 8 shows the average execution time of

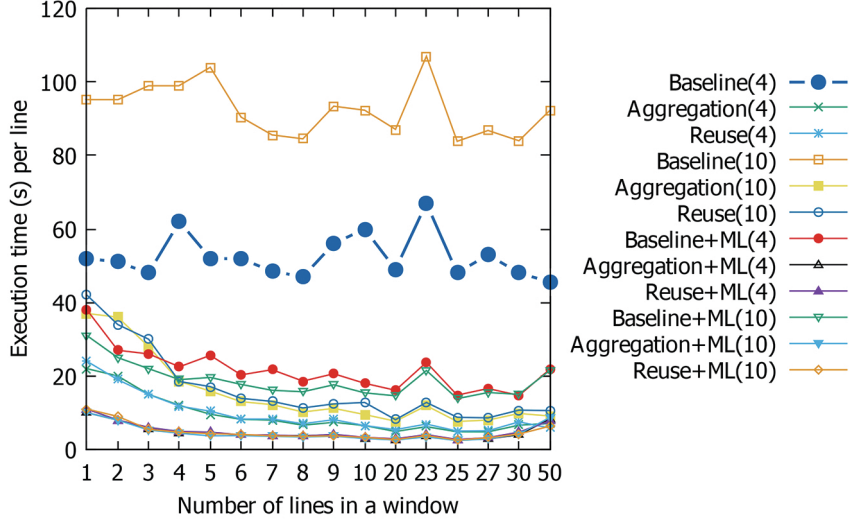


Figure 9: **Average execution time per line for PDF computation with two windows.** With 4 – *types* (4) and 10 – *types* (10).

PDF computation for different window sizes using Grouping. As shown in Figure 8, the average execution time of each line decreases for larger window sizes. This is reasonable because when the number of lines increases, more points are aggregated to each group so that more redundant calculations are avoided. When the window size is 25 lines, the average execution time of each line is minimal. From that point on, when the window size increases, the execution time also increases. This is expected since when the number of lines in a window increases, the time to shuffle data among different nodes increases more than the reduced time by avoiding redundant calculations. As a result, the average execution time of each line becomes more significant. However, the average execution time of data loading stays the same for different window sizes, *i.e.* about 12s per line.

We measure the execution time of PDF computation for different window sizes using other methods. In Figure 9, we can see that the window size of 25 is the optimal size for the other methods. In addition, the execution time of PDF computation is almost the same for different combinations of methods: Grouping plus ML and Reuse plus ML both with 4–*types* or 10–*types*. Baseline always corresponds to longer execution times of PDF computation. Compared with Baseline, Grouping, Reuse and ML can reduce the execution time up to 91% (more than 10 times faster) and 84% (more than 6 times faster). In addition, the combination of Grouping and ML can be up to 97% (more than 33 times) faster. This shows the obvious performance advantage of our methods in computing PDFs.

**Execution of One Slice** In this section, we compare the performance of different methods to execute the program for the points of the whole slice, *i.e.* Slice 201. We take 25 lines as the window size for PDF computation and execute the program with different methods the whole slice, *i.e.* 11 windows of points in Slice 201. The execution time of data loading is the same for the different methods, *i.e.* 4098s. The average execution time of each line is longer than that of the small workload since we cache all the data in memory during the execution of different methods and the time to store data increases as the amount of cached data grows. The execution time of PDF computation is shown in Figure 10 and the error is shown in 11.

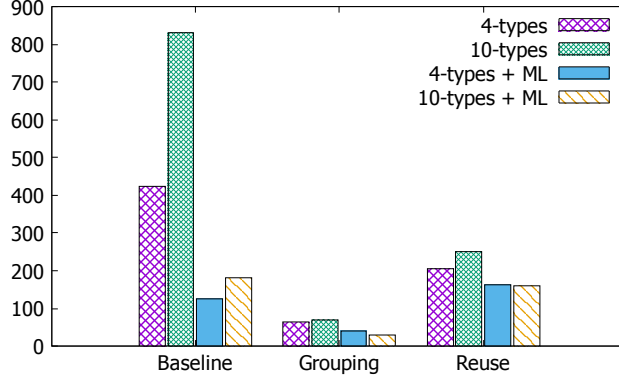


Figure 10: **Execution time of PDF computation of Slice 201 with different methods (235 GB input data).** The time unit is minute. The window size is 25 lines.

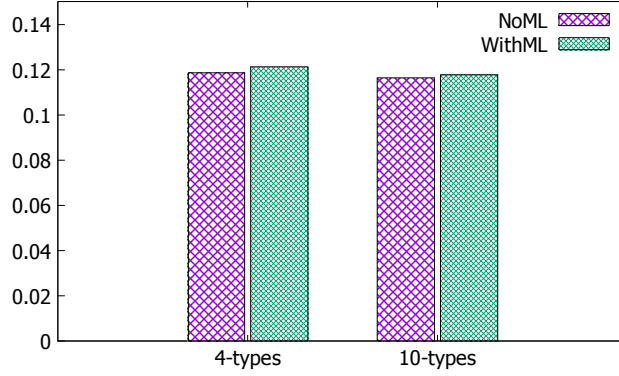


Figure 11: **Error in PDF computation.** NoML stands for Baseline, Grouping and Reuse plus 4 – type and 10 – types. WithML stands for Baseline + ML, Grouping + ML, Reuse + ML 4 – type and 10 – types.

Figure 10 shows that our proposed methods, *i.e.* Grouping, Reuse and ML, always outperform Baseline for both 4 – types and 10 – types. Grouping can reduce the execution time up to 92% (more than 10 times) and ML up to 78% (more than 3 times faster). The performance of Reuse is better than that of Baseline when we do not combine ML and the advantage can be up to 70% (more than 2 times faster). However, the performance of the combination of Reuse and ML can be worse than the combination of Baseline and ML. This is possible when it takes too much time to search for the existing results. The combination of Grouping and ML can reduce the execution time up to 97% (more than 27 times faster) compared with Baseline.

Figure 11 shows the error of PDF computation. The error is smaller than that of the small workload. The error of NoML is still smaller than that of WithML. The error for 4 – types is almost the same as that for 10 – types. But the error for 10 – types using ML is smaller than that for 4 – types. This is similar to what was observed when executing the small workload. In addition, the error for 10 – types with ML is even smaller than the error for 4 – types without ML. Although there is very small difference (up to 0.0016) of error between Baseline and ML, the execution time of the PDF computation process is largely reduce by ML.

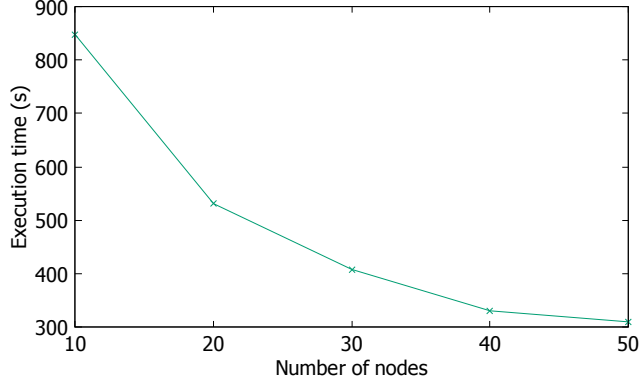


Figure 12: Execution time for data loading with different numbers of nodes.

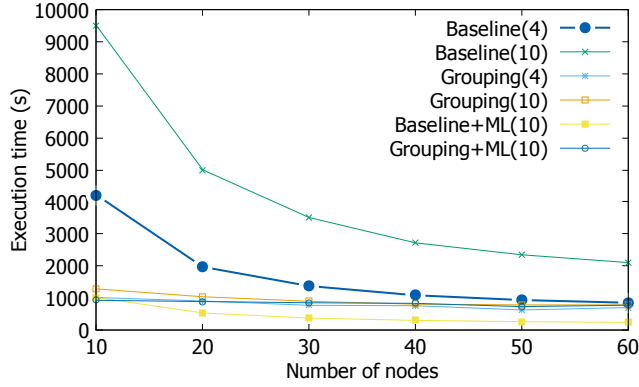


Figure 13: Execution time of PDF computation with different numbers of nodes.

### 6.2.2 Scalability Comparisons

In this section, we study the scalability of Baseline and the methods that have good performance, *i.e.* Grouping, ML and Grouping + ML. We use the G5k cluster with different numbers of nodes from 10 to 60.

The execution time of data loading with different methods remains the same for the same number of nodes. Figure 12 shows the execution time of data loading, which decreases rapidly as the number of nodes increases. This indicates the good scalability of our data loading process.

The execution time of PDF computation for different methods and different numbers of nodes is shown in Figure 13. We do not consider Reuse since it is less efficient than Grouping. We focus on ML for 10 – *types* because it has small error and an execution time similar to that for 4 – *types*. The figure shows that the execution time of Grouping and ML is always better than that of Baseline. The advantage of Grouping can be up to 87% (more than 6 times faster). ML outperforms Baseline up to 89% (more than 8 times faster). Grouping + ML can be better than Baseline by up to 90% (more than 9 times faster). In addition, the execution time of each method decreases as the number of nodes increases, which indicates that all methods have good scalability. However, the advantage becomes less obvious from 50 nodes on.

Figure 14 gives a focus on our methods. We do not compare the error of PDF computation since it is similar to that given in Section 6.2.1. The figure shows that Grouping + ML is better

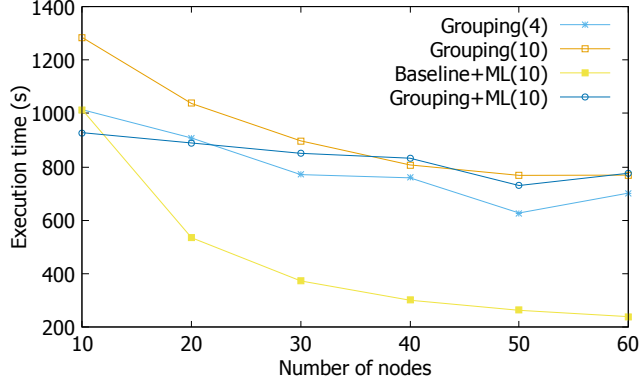


Figure 14: Execution time of PDF computation with different numbers of nodes and a focus on Grouping, ML, Baseline + ML and Grouping + ML.

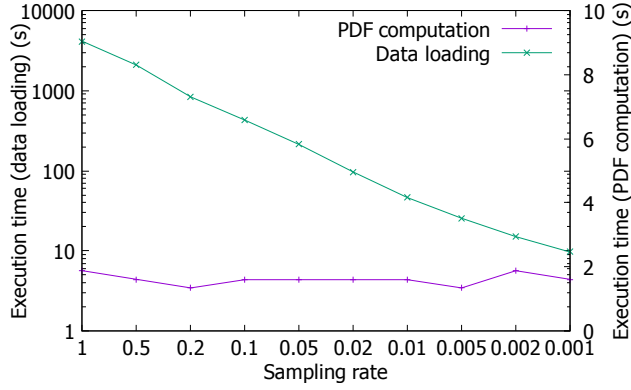


Figure 15: Execution time with different sampling rates using random sampling.

than either Grouping or ML when the number of nodes is 10. However, ML starts outperforming Grouping + ML when the number of nodes exceeds 10. This is because the shuffling of data among different nodes takes much time. As the number of nodes increases, the more time to transfer data among the nodes also increases. Thus, the performance of the aggregation function becomes a bottleneck for Grouping + ML when the number of nodes is high.

### 6.2.3 Performance of Sampling

We now study the efficiency of Sampling. We carried out the experiments in the LNCC cluster. We use two sampling methods, *i.e.* random sampling and k-means clustering (see Section 5.4). We compare the performance of the two sampling method with different sampling rates.

Figure 15 shows the execution time of random sampling with different sampling rates. The execution time for data loading decreases almost linearly as the sampling rate decreases (both the X and Y axis use a base-10 log scale). This is reasonable since when the sampling rate gets small, the data loading needs to process less points and thus loads less data. The execution time for PDF computation is very short (about 2 seconds). This is expected since we avoid calling the R program to compute PDFs and use a decision tree model to predict the distribution type of each point. The execution time is almost the same for different sampling rates since it is already

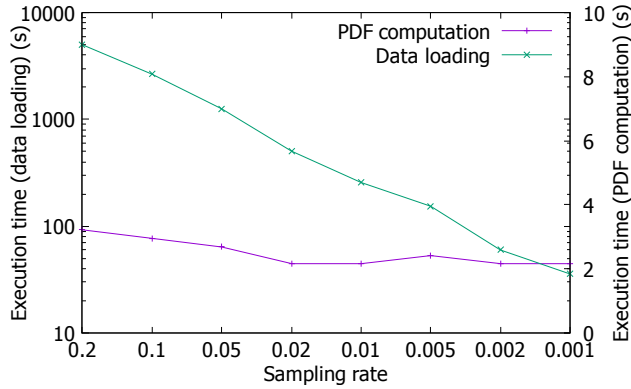


Figure 16: Execution time with different sampling rates using k-means sampling.

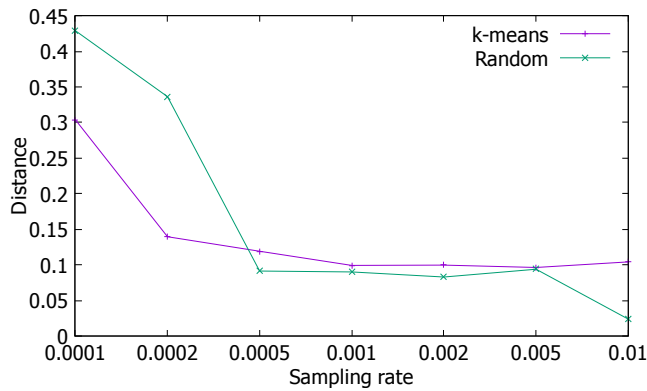


Figure 17: Distance of the distribution type percentage between the double sampled points and all points.

very short and data shuffling also takes some time. In addition, we only need to transfer the mean and standard deviation values instead of the whole data set for the prediction, which also reduces time. This execution time is about 2 seconds, which is very short. However, this method cannot calculate the error of the PDF computation process. It can help to have a general view of the whole slice. Then a slice is chosen to compute the PDFs of the corresponding points.

Figure 16 shows the performance of k-means clustering for sampling the points. The results are almost the same as that of random sampling, *i.e.* the execution time for data loading decreases linearly and the execution time for PDF computation is very short and almost the same for different sampling rates. The execution time of k-means is longer than that of random for the same sampling rate. We measure the sampling rate from 0.2 since the corresponding execution time of k-means for data loading is already longer than that of random sampling with the sampling rate of 1.

Figure 17 shows the Euclidean distance of the distribution type percentage between the double sampled points and all points in one slice using k-means and random sampling. When the sampling rate is small, the result of k-means is close to the percentage of overall points. This is because the double sampled points of k-means method contain diverse information. However, when the sampling rate is high, the results of random sampling are similar or better since enough



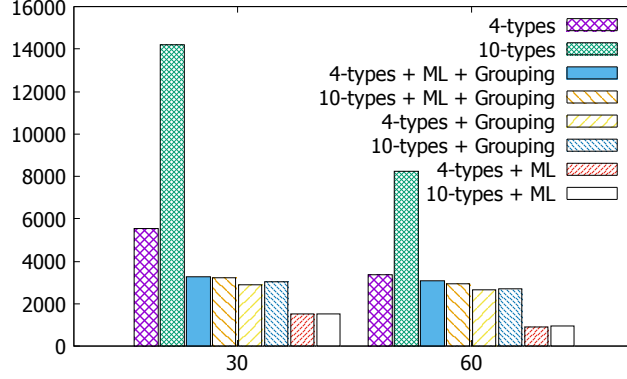


Figure 18: **Execution time for all the points in Slice 201 (1.9 TB input data).** The time unit is second.

points are selected with a high sampling rate. Since random sampling is faster than k-means, we choose it in the following experiments.

### 6.3 Experiments on Big Data Sets

In this section, we compare the performance of different methods based on big spatial data sets of several TB, *i.e.* *Set2* and *Set3* (see details in Section 6.1). We use the G5k cluster with 30 and 60 nodes.

#### 6.3.1 Experiments with 1000 Simulations

In this section, we perform experiments using *Set2* of 1.9 TB generated by 1000 simulations. We take the relationship between the combination of mean and standard deviation values and the distribution types of 25000 points in Slice 0 as previously generated data to build the decision tree model. The model error of 4 – *types* is 0.02 and the model error of 10 – *types* is 0.09. The time to load the model ranges between 1 and 20 seconds, which is negligible compared with the execution time of PDF computation. The time for data loading is 2671 seconds with 30 nodes and 1619 seconds with 60 nodes, which shows the good scalability of the data loading process.

Figure 18 shows the good performance of our methods, *i.e.* Grouping and ML. Grouping is better than Baseline (up to 79%) but not as good as ML, because of data shuffling with many nodes. And the scalability of Grouping is not good. ML largely outperforms Baseline (up to 89%) and has good scalability. Because of the shuffling bottleneck, the combination of Grouping and ML is worse than ML but still better (up to 77%) than Baseline. The error of ML with 10 – *types* is always smaller than with 4 – *types*.

Finally, we experimented with random sampling to process the data in two clusters of 30 and 60 nodes. The execution time of PDF computation ranges between 260s and 280s while the sampling rate ranges between 0.001 and 1. The average execution time (272s for 30 nodes and 266 for 60 nodes) is 82% and 71% shorter than the minimum execution time (ML with 4 – *types* for 30 and 60 nodes) shown in Figure 18. Note that doubling the number of nodes does not yield much improvement. This is because using more nodes increases data transfers to send the mean and standard deviation values and the distribution type from each node to the Spark master node in Spark cluster to compute the distribution percentage.

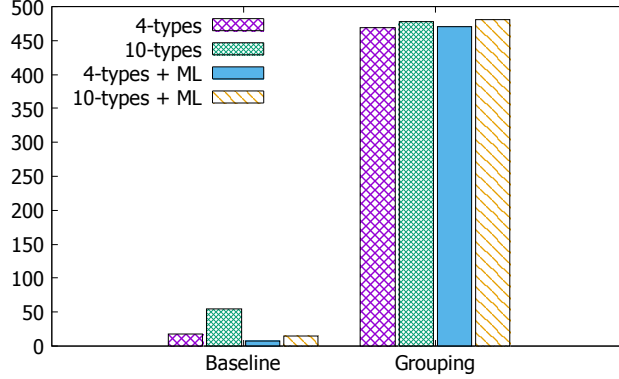


Figure 19: Execution time for PDF computation on small workload (2 lines and 1002 points) with 2.4 TB input data. The time unit is second.

### 6.3.2 Experiments with 10000 Simulations

In this section, we perform experiments using *Set3* of 2.4 TB generated by 10000 simulations. Again, we take the relationship between the combination of mean and standard deviation values and the distribution types of 25000 points in Slice 0 as the previously generated data for the decision tree model. The model error of 4 – *types* is 0.006 and the model error of 10 – *types* is 0.012. The time to load the model ranges between 1 and 20 seconds, which is negligible compared with the execution time of PDF computation. First, we execute the program for the points of the first 2 lines in Slice 201 in a cluster of 30 nodes. We take 1 line as a window, and we process the data of two windows. The execution time for data loading (Algorithm 2) is 28s, which is the same for all the methods since we use the same algorithm (Algorithm 2). The execution time for PDF computation is shown in Figure 19.

Figure 19 shows the superior performance of ML. The execution time of Baseline with 10 – *types* is much longer than that of 4 – *types* as expected. Compared with Baseline, ML reduces execution time much (57% with 4 – *types* and 72% with 10 – *types*). However, the execution time of Grouping is much longer. This is because the data size of each point is 9 times bigger since a point corresponds to 10000 observation values instead of 1000. During Grouping, much more data is transferred among different nodes, which takes much time. Thus, in the next experiment, we do not use Grouping.

We also measure the error ( $E$  defined in Equation 6) during execution. 10 – *types* does not reduce much the average error for Baseline (up to 0.008). However, it may take much more time for PDF computation when we consider 10 – *types* as shown in Figure 19. Using WithML, the average error is slightly bigger than that of NoML. The difference is very small (up to 0.007) but ML can reduce much the execution time of PDF computation. Furthermore, 10 – *types* leads to smaller average error even though the model error is bigger when using ML.

Now, we execute the program for all points in Slice 201. As we only compare the execution with Baseline and ML, we take 126 lines as a window in order to parallelize the execution of different points in different nodes. The time for data loading is 4592 seconds with 30 nodes. Figure 20 shows the superior performance of ML (up to 88%, *i.e.* more than 7 times faster than Baseline). Furthermore, the PDF computation process scales very well. We measured the average error and found that ML incurs small error while reducing execution time much. Finally, we use the random sampling to process the data in two clusters of 30 and 60 nodes. The execution time of PDF computation ranges between 128s and 200s while the sampling rate

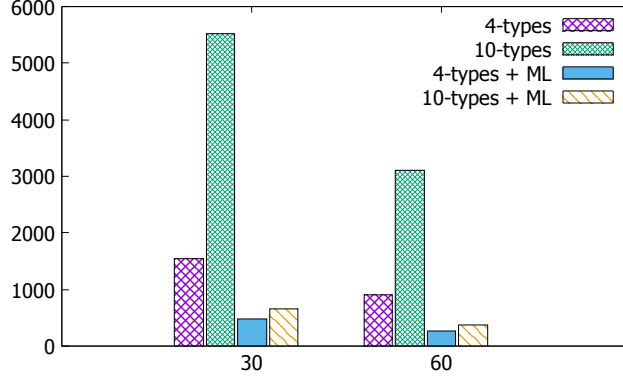


Figure 20: **Execution time for all the points in Slice 201 (2.4 TB input data).** The time unit is second.

ranges between 0.001 and 1. The average execution time (172s for 30 nodes and 155s for 60 nodes) is 64% and 41% smaller than the minimum execution time (ML with 4 – *types* for 30 and 60 nodes) shown in Figure 20. Again (as for the experiment with 1000 simulations), doubling the number of nodes does not yield much improvement.

## 7 Conclusion

Uncertainty quantification of spatial data requires computing a Probability Density Function (PDF) of each point in a spatial cube area. However, computing PDFs on big spatial data, as produced by applications in scientific areas such as geological or seismic interpretation, can be very time consuming.

In this paper, we addressed the problem of efficiently computing PDFs under bounded error constraints. We proposed a parallel solution using a Spark cluster with three new methods: Grouping, ML and Sampling. Grouping aggregates the points of the same statistical features together in order to reduce redundant calculation. This method is very efficient when the data to be transferred is not too big and the number of cluster nodes is small. ML generates a decision tree model based on previously generated data and predicts the distribution type of a point in order to avoid useless calculation based on wrong distribution types. Sampling enables to efficiently compute statistical parameters of a region by sampling a fraction of the total number of points to reduce the computation space.

To validate our solution, we implemented these methods in a Spark cluster and performed extensive experiments on two different computer clusters (with 6 and 64 nodes) using big spatial data ranging from hundreds of GB to several TB. This data was generated from simulations based on the models from a seismic benchmark for oil and gas exploration, which includes models for seismic wave propagation.

The experimental results show that our solution is efficient and scales up very well compared with Baseline. Grouping outperforms Baseline by up to 92% (more than 10 times) without introducing extra error. ML can be up to 91% (more than 9 times) better than Baseline with very slight acceptable error (up to 0.017). The combination of Grouping and ML can be up to 97% (more than 33 times) better than Baseline. As the number of nodes exceeds 10 nodes, ML outperforms the combination. Thus, in order to compute PDFs, the combination of Grouping and ML is the optimal method when each point corresponds to a small number of observation

values, e.g. 1000, and when there is small number of nodes (less than 20). Otherwise, ML is the best option. We also showed that Sampling is very efficient to calculate general statistics information in order to choose a slice for calculating PDFs. Finally, Sampling should be used with the aforementioned best option in order to efficiently compute PDFs.

## Acknowledgment

This work was partially funded by EU H2020 Project HPC4e with MCTI/RNP-Brazil, CNPq, FAPERJ, and Inria Associated Team SciDISC. The work of J. Liu, E. Pacitti and P. Valduriez were performed in the context of the Computational Biology Institute (<http://www.ibr-montpellier.fr>). The experiments were carried out using a cluster at LNCC in Brazil and the Grid5000 testbed in France (<https://www.grid5000.fr>).

## References

- [1] Hpc geophysical simulation test suite. <https://hpc4e.eu/downloads/hpc-geophysical-simulation-test-suite>.
- [2] Spark MLlib. <https://spark.apache.org/mllib/>.
- [3] R. Belohlávek, B. D. Baets, J. Outrata, and V. Vychodil. Inducing decision trees via concept lattices. *Int. Journal of General Systems*, 38(4):455–467, 2009.
- [4] R. Campisano, F. Porto, E. Pacitti, F. Masegla, and E. S. Ogasawara. Spatial sequential pattern mining for seismic data. In *Simpósio Brasileiro de Banco de Dados (SBBD)*, pages 241–246, 2016.
- [5] M. Chen, S. Mao, and Y. Liu. Big data: A survey. *Mobile Networks and Applications*, 19(2):171–209, 2014.
- [6] N. Cressie. *Statistics for spatial data*. John Wiley & Sons, 2015.
- [7] J. Dean and S. Ghemawat. Mapreduce: Simplified data processing on large clusters. In *Symp. on Operating System Design and Implementation (OSDI)*, pages 137–150, 2004.
- [8] W. J. Dixon and F. J. Massey. *Introduction to statistical analysis*. 1968.
- [9] S. Fotheringham, C. Brunson, and M. Charlton. *Quantitative Geography: Perspectives on Spatial Data Analysis*. 2000.
- [10] S. Ghemawat, H. Gobioff, and S. Leung. The google file system. In *ACM Symp. on Operating Systems Principles (SOSP)*, pages 29–43, 2003.
- [11] E. R. Harold. *Java I/O: Tips and Techniques for Putting I/O to Work*, pages 131–132. 2006.
- [12] T. J. Jackson, D. M. L. Vine, A. Y. Hsu, A. Oldak, P. J. Starks, C. T. Swift, J. D. Isham, and M. Haken. Soil moisture mapping at regional scales using microwave radiometry: the southern great plains hydrology experiment. *IEEE Transactions Geoscience and Remote Sensing*, 37(5):2136–2151, 1999.

- [13] F. Kathryn, J. T. Oden, and D. Faghihi. A bayesian framework for adaptive selection, calibration, and validation of coarse-grained models of atomistic systems. *Journal of Computational Physics*, 295:189 – 208, 2015.
- [14] S. Landset, T. M. Khoshgoftaar, A. N. Richter, and T. Hasanin. A survey of open source tools for machine learning with big data in the hadoop ecosystem. *Journal of Big Data*, 2(1):24, 2015.
- [15] J. Liu, E. Pacitti, and P. Valduriez. A survey of scheduling frameworks in big data systems. *International Journal of Cloud Computing*, page 27, 2018.
- [16] R. H. C. Lopes. Kolmogorov-smirnov test. In *Int. Encyclopedia of Statistical Science*, pages 718–720, 2011.
- [17] S. Marelli and B. Sudret. Uqlab: A framework for uncertainty quantification in matlab. In *Int. Conf. on Vulnerability, Risk Analysis and Management (ICVRAM)*, pages 2554–2563, 2014.
- [18] X. Meng, J. Bradley, B. Yavuz, E. Sparks, S. Venkataraman, D. Liu, J. Freeman, D. Tsai, M. Amde, S. Owen, D. Xin, R. Xin, M. J. Franklin, R. Zadeh, M. Zaharia, and A. Talwalkar. MLlib: Machine Learning in Apache Spark. *Journal of Machine Learning Research*, 17(34):1–7, 2016.
- [19] C. Michele, T. Stefano, and S. Andrea. Sensitivity and uncertainty analysis in spatial modelling based on gis. *Agriculture, Ecosystems & Environment*, 81(1):71 – 79, 2000.
- [20] S. R. Safavian and D. Landgrebe. A survey of decision tree classifier methodology. *IEEE Transactions on Systems, Man, and Cybernetics*, 21(3):660–674, 1991.
- [21] R. Sandberg, D. Goldberg, S. Kleiman, D. Walsh, and B. Lyon. Design and implementation of the sun network file system. In *the Summer USENIX conf.*, pages 119–130, 1985.
- [22] K. Shvachko, H. Kuang, S. Radia, and R. Chansler. The hadoop distributed file system. In *IEEE Symp. on Mass Storage Systems and Technologies (MSST)*, pages 1–10, 2010.
- [23] P. Snyder. tmpfs: A virtual memory file system. In *European UNIX Users Group Conf.*, pages 241–248, 1990.
- [24] G. Trajcevski. Uncertainty in spatial trajectories. In *Computing with Spatial Trajectories*, pages 63–107, 2011.
- [25] F. Wang and J. Liu. Networked wireless sensor data collection: Issues, challenges, and approaches. *IEEE Communications Surveys and Tutorials*, 13(4):673–687, 2011.
- [26] B. Zadrozny and C. Elkan. Obtaining calibrated probability estimates from decision trees and naive bayesian classifiers. In *Int. Conf. on Machine Learning (ICML)*, pages 609–616, 2001.
- [27] M. Zaharia, M. Chowdhury, M. J. Franklin, S. Shenker, and I. Stoica. Spark: Cluster computing with working sets. In *USENIX Workshop on Hot Topics in Cloud Computing (HotCloud)*, 2010.